Center for Infection and Inflammation Imaging Research
Johns Hopkins University School of Medicine

Pathogen Specific PET/CT Imaging for Gram Negative Implant Associated Spinal Infections

Oren Gordon[1,2], Anna Napiorkowski[1,2], Kelly Flavahan[1,2], Trisha De Jesus[1,2], Dustin A. Dikeman[3], Amy Kronenberg[1,2], Nathan K. Archer[3] and Sanjay K. Jain[1,2,4]

[1]Division of Infectious Diseases, Department of Pediatrics, [2]Center for Infection and Inflammation Imaging Research, [3]Department of Dermatology, and [4]Division of Nuclear Medicine and Molecular Imaging, Russell H. Morgan Department of Radiology and Radiological Science, Johns Hopkins University School of Medicine, Baltimore, MD, USA.

Introduction

Rapid and accurate diagnosis of bacterial implant-associated spinal infection is essential for early intervention, surgical planning and rational use of antibiotics. While this infection is predominantly caused by Gram positive bacteria, some patients are at high risk for intestinal-derived Gram-negative bacteria. However, current diagnostic tools require invasive sampling with substantial risks to the patient. Moreover, conventional imaging, including computed tomography (CT), magnetic resonance imaging (MRI) and positron emission tomography (PET) with 2-deoxy-2-[^{18}F]fluoro-D-glucose (^{18}F-FDG), cannot differentiate infection from non-infectious processes.

Methods

PET/CT with 2-deoxy-2-[^{18}F]fluoro-D-sorbitol (^{18}F-FDS) is the first imaging modality specific for a bacterial class. ^{18}F-FDS accumulates selectively in *Enterobacterales*, but not in Gram positive bacteria or mammalian cells and was safe in phase I-II clinical studies. Here, we developed a spinal infection model utilizing a previously described posterior-approach to implant a titanium Kirschner wire into the L4 spinous process in mice. We compared ^{18}F-FDS with ^{18}F-FDG PET/CT in mice with spinal implants infected with *Staphylococcus aureus* (Figure 1), *Escherichia coli* (Figure 2) or without infection (but with post-surgical inflammation).

Results

Both bacteria induced substantial bone pathology with reduced bone density (Figure 2D). ^{18}F-FDS PET/CT could specifically detect implant-associated spinal infections due to *E. coli* with mean target-to-non-target standard uptake value (SUV) ratio of 9.2 ± 1.5, which was substantially lower in *S. aureus* (3.0 ± 0.4) and uninfected mice (4.3 ± 0.3; *P*=0.002; Figure 3). In contrast, ^{18}F-FDG could not differentiate between the two bacterial infections or the controls (*P*=0.497; Figure 4). Finally, ^{18}F-FDS monitored the efficacy of antibiotic treatment, demonstrating a signal proportional to bacterial burden (Figure 5).

Conclusion

In this preclinical study, ^{18}F-FDS PET/CT rapidly and specifically detected *E.coli* implant-associated spinal infection. We are currently conducting a clinical study to evaluate ^{18}F-FDS PET/CT for specific detection of *Enterobacterales* implant-associated infection which may reduce the need for surgical interventions.

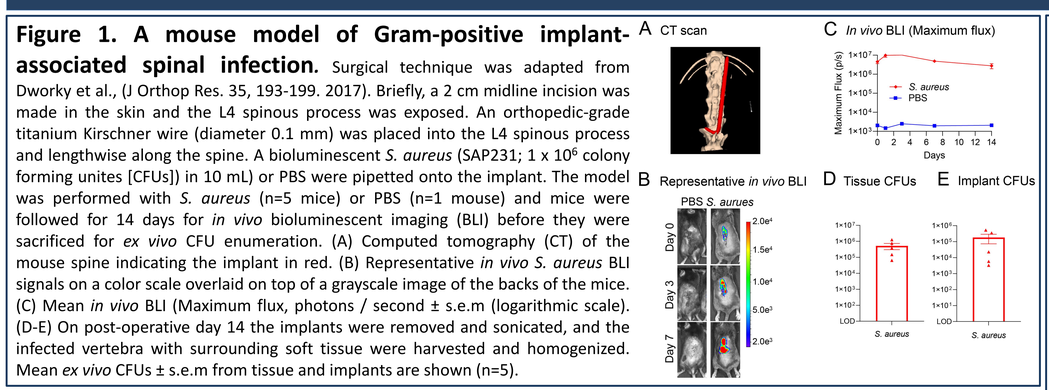

Figure 1. A mouse model of Gram-positive implant-associated spinal infection. Surgical technique was adapted from Dworky et al., (J Orthop Res. 35, 193-199. 2017). Briefly, a 2 cm midline incision was made in the skin and the L4 spinous process was exposed. An orthopedic-grade titanium Kirschner wire (diameter 0.1 mm) was placed into the L4 spinous process and lengthwise along the spine. A bioluminescent *S. aureus* (SAP231; 1 x 10^6 colony forming unites [CFUs]) in 10 mL) or PBS were pipetted onto the implant. The model was performed with *S. aureus* (n=5 mice) or PBS (n=1 mouse) and mice were followed for 14 days for *in vivo* bioluminescent imaging (BLI) before they were sacrificed for *ex vivo* CFU enumeration. (A) Computed tomography (CT) of the mouse spine indicating the implant in red. (B) Representative *in vivo S. aureus* BLI signals on a color scale overlaid on top of a grayscale image of the backs of the mice. (C) Mean *in vivo* BLI (Maximum flux, photons / second ± s.e.m (logarithmic scale). (D-E) On post-operative day 14 the implants were removed and sonicated, and the infected vertebra with surrounding soft tissue were harvested and homogenized. Mean *ex vivo* CFUs ± s.e.m from tissue and implants are shown (n=5).

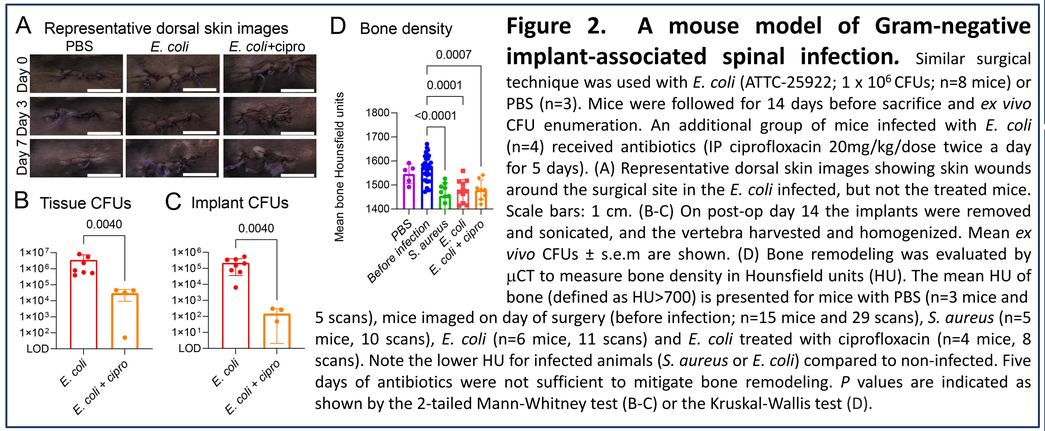

Figure 2. A mouse model of Gram-negative implant-associated spinal infection. Similar surgical technique was used with *E. coli* (ATTC-25922; 1 x 10^6 CFUs; n=8 mice) or PBS (n=3). Mice were followed for 14 days before sacrifice and *ex vivo* CFU enumeration. An additional group of mice infected with *E. coli* (n=4) received antibiotics (IP ciprofloxacin 20mg/kg/dose twice a day for 5 days). (A) Representative dorsal skin images showing skin wounds around the surgical site in the *E. coli* infected, but not the treated mice. Scale bars: 1 cm. (B-C) On post-op day 14 the implants were removed and sonicated, and the vertebra harvested and homogenized. Mean *ex vivo* CFUs ± s.e.m are shown. (D) Bone remodeling was evaluated by µCT to measure bone density in Hounsfield units (HU). The mean HU of bone (defined as HU>700) is presented for mice with PBS (n=3 mice and 5 scans), mice imaged on day of surgery (before infection; n=15 mice and 29 scans), *S. aureus* (n=5 mice, 10 scans), *E. coli* (n=6 mice, 11 scans) and *E. coli* treated with ciprofloxacin (n=4 mice, 8 scans). Note the lower HU for infected animals (*S. aureus* or *E. coli*) compared to non-infected. Five days of antibiotics were not sufficient to mitigate bone remodeling. *P* values are indicated as shown by the 2-tailed Mann-Whitney test (B-C) or the Kruskal-Wallis test (D).

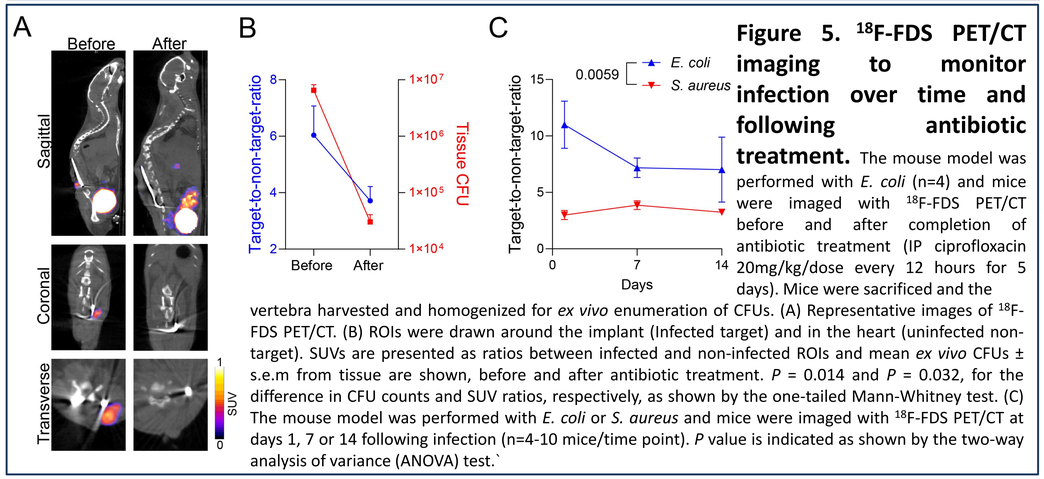

Figure 5. ^{18}F-FDS PET/CT imaging to monitor infection over time and following antibiotic treatment. The mouse model was performed with *E. coli* (n=4) and mice were imaged with ^{18}F-FDS PET/CT before and after completion of antibiotic treatment (IP ciprofloxacin 20mg/kg/dose every 12 hours for 5 days). Mice were sacrificed and the vertebra harvested and homogenized for *ex vivo* enumeration of CFUs. (A) Representative images of ^{18}F-FDS PET/CT. (B) ROIs were drawn around the implant (Infected target) and in the heart (uninfected non-target). SUVs are presented as ratios between infected and non-infected ROIs and mean *ex vivo* CFUs ± s.e.m from tissue are shown, before and after antibiotic treatment. *P* = 0.014 and *P* = 0.032, for the difference in CFU counts and SUV ratios, respectively, as shown by the one-tailed Mann-Whitney test. (C) The mouse model was performed with *E. coli* or *S. aureus* and mice were imaged with ^{18}F-FDS PET/CT at days 1, 7 or 14 following infection (n=4-10 mice/time point). *P* value is indicated as shown by the two-way analysis of variance (ANOVA) test.`

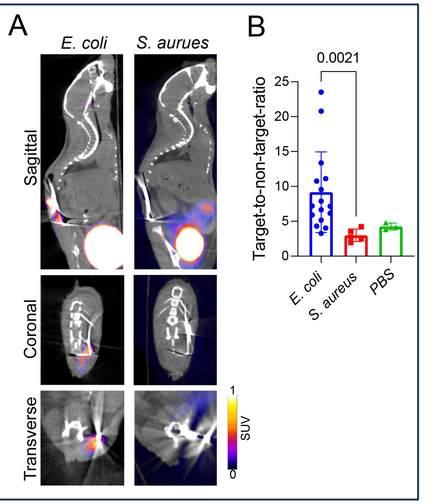

Figure 3. ^{18}F-FDS PET/CT imaging for detection of Gram-negative implant associated spinal infection in mice. The mouse model was performed with either *E. coli* (n=15), *S. aureus* (n=5) or PBS (n=3) and mice were imaged with ^{18}F-FDS PET/CT imaging. (A) Representative images of ^{18}F-FDS PET/CT. (B) Regions of interest (ROIs) were drawn around the implant (Infected target) and in the heart (uninfected non-target). Standard uptake values (SUVs) are presented as ratios between infected and non-infected ROIs. *P* values are indicated as shown by the Kruskal-Wallis test adjusted for multiple comparisons to preserve the desired false discovery rate.

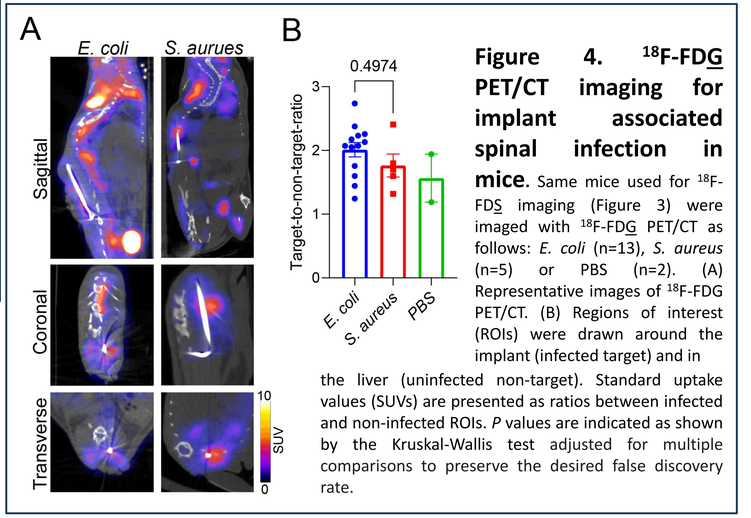

Figure 4. ^{18}F-FDG PET/CT imaging for implant associated spinal infection in mice. Same mice used for ^{18}F-FDS imaging (Figure 3) were imaged with ^{18}F-FDG PET/CT as follows: *E. coli* (n=13), *S. aureus* (n=5) or PBS (n=2). (A) Representative images of ^{18}F-FDG PET/CT. (B) Regions of interest (ROIs) were drawn around the implant (infected target) and in the liver (uninfected non-target). Standard uptake values (SUVs) are presented as ratios between infected and non-infected ROIs. *P* values are indicated as shown by the Kruskal-Wallis test adjusted for multiple comparisons to preserve the desired false discovery rate.

Questions? Please reach out!
Current affiliation: Oren Gordon, Hadassah-Hebrew University Medical Center, Jerusalem, Israel, orengo@hadassah.org.il.

@SanjayJain_Lab
@gordon_oren

Funded by the National Institute of Health grant R01-EB025985 and Department of Defense grant W81XWH-18-1-0642.